ISSN 0023-1584, Kinetics and Catalysis, 2009, Vol. 50, No. 5, pp. 725–733. © Pleiades Publishing, Ltd., 2009.
Original Russian Text © A.V. Vosmerikov, V.I. Zaikovskii, L.L. Korobitsyna, G.V. Echevskii, V.V. Kozlov, Ya.E. Barbashin, S.P. Zhuravkov, 2009, published in Kinetika i Kataliz, 2009, Vol. 50, No. 5, pp. 755–763.

Nonoxidative Conversion of Methane into Aromatic Hydrocarbons on Ni–Mo/ZSM-5 Catalysts

A. V. Vosmerikov[a], V. I. Zaikovskii[b], L. L. Korobitsyna[a], G. V. Echevskii[b], V. V. Kozlov[a], Ya. E. Barbashin[a], and S. P. Zhuravkov[c]

[a] *Institute of Petroleum Chemistry, Siberian Branch, Russian Academy of Sciences, Tomsk, 634055 Russia*
[b] *Boreskov Institute of Catalysis, Siberian Branch, Russian Academy of Sciences, Novosibirsk, 630090 Russia*
[c] *Research Institute of High-Voltage Equipment, Tomsk Polytechnic University, Tomsk, Russia*
e-mail: pika@ipc.tsc.ru

Received July 7, 2008

Abstract—The nonoxidative conversion of methane into aromatic hydrocarbons on high-silica zeolites ZSM-5 containing nanosized powders of molybdenum (4.0 wt %) and nickel (0.1–2.0 wt %) was studied. Data on the acid characteristics of the catalysts and the nature and amount of coke deposits formed on the surface of the catalysts were obtained using the thermal desorption of ammonia and thermal analysis. The microstructure and composition of Ni–Mo/ZSM-5 catalysts were studied by high-resolution transmission electron microscopy and energy-dispersive X-ray analysis. The formation of various chemical species in the samples was detected: oxide-like clusters of Mo within zeolite channels (~1 nm), molybdenum carbide particles (5–30 nm) on the outer surface of the zeolite, and Ni–Mo alloy particles with different compositions (under reaction conditions, carbon filaments grew on these particles). It was found that, as the Ni content was increased from 0.1 to 2.0 wt %, the rate of deactivation of the catalytic system increased because of blocking pores in the zeolite structure by filamentous carbon up to the formation of condensed coke deposits.

DOI: 10.1134/S0023158409050140

INTRODUCTION

Methane dehydroaromatization under nonoxidative conditions on zeolite catalysts modified with transition metal ions is a promising process for the efficient utilization of natural gas and casing-head gas. A disadvantage of this process, which occurs at high temperatures (700–800°C), is rapid catalyst deactivation because of intense coke formation. To increase the time of stable catalyst operation in methane dehydroaromatization, the catalysts are modified with various metals (Y, Cu, Zr, La, Pt, and Fe) [1–4]. In this work, we studied the modifying effect of nickel on the catalytic properties of molybdenum-containing zeolite ZSM-5 in the methane dehydroaromatization reaction. The formation of coke on the surface of Ni–Mo/ZSM-5 catalysts in the course of the reaction was studied and its structure and concentration were determined using thermal analysis and high-resolution transmission electron microscopy (HP TEM).

EXPERIMENTAL

Catalysts were prepared by mechanically mixing zeolite ZSM-5 with the molar ratio $SiO_2/Al_2O_3 = 40$ and the nanosized powders of Mo and Ni in a KM-1 vibratory ball mill (Germany) for 4 h. Thereafter, the resulting mixtures were calcined at 540°C for 6 h. The nanopowders of Mo and Ni were prepared by the method of electrical explosion of wires in an atmosphere of argon [5]. The concentration of Mo in the zeolite was 4.0 wt %, and the concentration of Ni in the 4.0% Mo/ZSM-5 catalytic system was varied from 0.1 to 2.0 wt %.

The nonoxidative conversion of methane (99.9% purity) was performed in a flow setup at 750°C and atmospheric pressure. A catalyst sample (1.0 cm^3) was placed in a quartz tube reactor 12 mm in diameter. Before the onset of reaction, the catalyst was heated to 750°C in a flow of helium and kept for 20 min at this temperature; thereafter, methane was supplied at a space velocity of 1000 h^{-1}. The reaction products were determined by gas chromatography. The acid characteristics of the samples were studied by the temperature-programmed desorption (TPD) of ammonia, which allowed us to determine the strength distribution and concentration of acid sites.

The formation and nature of coke deposits were studied by thermal analysis on a Derivatograph C (MOM, Hungary) over the temperature range of 20–800°C. A sample (400–500 mg), in a platinum crucible, was heated in air at a rate of 10 K/min (the sensitivity was 100 mg).

HRTEM images were obtained on a JEM-2010 electron microscope (JEOL, Japan) with a lattice resolution of 0.14 nm at an accelerating voltage of 200 kV. The high-resolution images of regular structures were

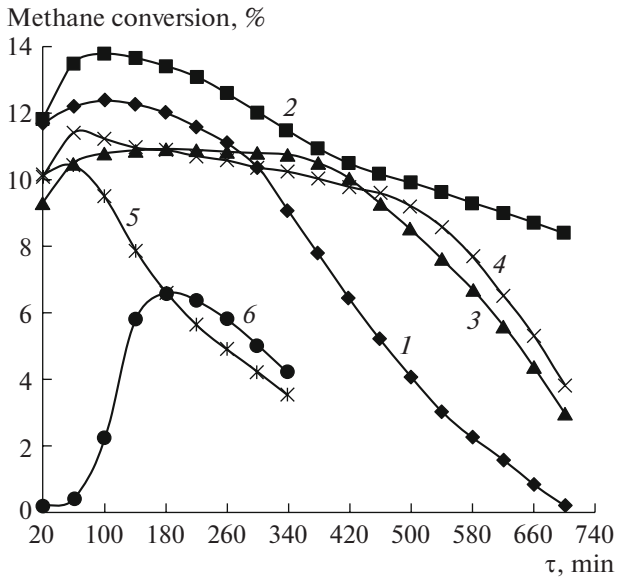

Fig. 1. Dependence of the conversion of methane on the time of methane dehydroaromatization on Mo/ZSM-5 with various nickel nanopowder contents: (*1*) initial 4.0% Mo/ZSM-5 and (*2*) 0.1, (*3*) 0.25, (*4*) 0.5, (*5*) 1.0, or (*6*) 2.0% Ni ($T = 750$°C; $W = 1000$ h^{-1}).

analyzed using the Fourier method. Energy-dispersive X-ray analysis (EDX) on an EDAX spectrometer (EDAX Co.) equipped with a Si(Li) detector with an energy resolution of no worse than 130 eV was used to perform the local elemental analysis of the samples. The samples for HRTEM were prepared on perforated carbon substrates fixed on copper gauzes.

RESULTS AND DISCUSSION

Figure 1 illustrates the effects of the concentration of the nanosized Ni powder and the reaction time of methane dehydroaromatization (τ) on the methane conversion and the stability of catalysts.

It can be seen that the addition of 0.1% Ni resulted in a considerable increase in the time of stable catalyst operation: after τ = 700 min, the conversion of methane was 8.6%, whereas the initial sample completely lost its activity in this time. The 4.0% Mo/ZSM-5 catalyst containing 0.1% Ni continued to exhibit activity after τ = 1020 min: the conversion was 3.6%.

The catalyst containing 0.5% Ni was found less active and stable that the sample of 0.1% Ni–4.0% Mo/ZSM-5, although it was more stable than the parent Mo/ZSM-5 catalyst. After the addition of 1.0 and 2.0% Ni nanopowder, the activity and stability of the 4.0% Mo/ZSM-5 catalyst dramatically decreased. On the sample of 2.0% Ni–4.0% Mo/ZSM-5, the maximum methane conversion was 6.6% after τ = 180 min. This catalyst almost did not exhibit catalytic activity in the first minutes of operation (the conversion was as low as 0.2–0.3%), and it was characterized by the longest induction period. It is likely that this behavior of the samples containing a relatively large amount of nickel oxide was due to the fact that a considerable portion of this oxide was reduced to nickel metal (which is characterized by high activity in coke formation) under the action of a reducing atmosphere. It is well known that nickel metal particles catalyze the growth of carbon filaments [6], which interlaced and curled to form numerous coils capable of deactivating the catalyst upon accumulation in a large amount.

The analysis of the composition of gaseous products formed upon methane conversion on the Ni–Mo-containing zeolites demonstrated that the yields of ethane and ethylene gradually increased in the course of reaction (Table 1). The amount of ethane formed on the samples containing Ni nanopowder was comparable to the amount formed on the sample with no nickel, whereas the amount of ethylene formed on the Ni-containing catalysts was much smaller; this was especially noticeable with increasing τ. Thus, after τ = 500 min, the yield of ethylene on the sample of 4.0% Mo/ZSM-5 was 0.83%, which is two times greater than that on the catalyst containing 0.1% Ni nanopowder.

On the catalysts with low Ni contents, as well as on the sample of 4.0% Mo/ZSM-5, benzene and naphthalene were formed in greater and smaller amounts, respectively, in the course of the entire experiment. The benzene/naphthalene ratio varied over a wide range in the course of reaction; however, in the majority of cases, it was close to 2. The yield of naphthalene was higher than the yield of benzene only on the sample of 1.0% Ni–4.0% Mo/ZSM-5 in the first 100 min of reaction; however, the fraction of benzene in the products then became greater than the amount of naphthalene as τ increased. On a less active sample of 2.0% Ni–4.0% Mo/ZSM-5, the yield of benzene was much greater than the yield of naphthalene at all τ.

Thus, note that the further addition of 0.1–0.5% of Ni nanopowder to the Mo-containing zeolite ZSM-5 was effective, and it allowed us to considerably increase the time of stable catalyst operation. It is likely that the role of nickel in the zeolite was related to the following functions: first, it regulated the degree of reduction of MoO_3 in accordance with the reaction $Ni^{2+} + Mo^{6+} \leftrightarrow Ni^{3+} + Mo^{5+}$ and thereby prevented the formation of a low-activity phase of $Al_2(MoO_4)_3$; second, it decreased the rate of formation of coke because of an enhanced hydrogenating capacity.

With consideration for a bifunctional mechanism of methane dehydroaromatization due to the participation of both Mo-containing active centers and the Brønsted acid sites of ZSM-5 [7, 8], it was of interest to study the effect of Ni nanopowder additives on the acid properties of both the unmodified and Mo-containing zeolites. From data given in Table 2, it follows that an increase in the concentration of nickel introduced into the parent zeolite from 0.1 to 0.5% did not result in a considerable change in the strength of acid sites, although a decrease in the concentrations of

Table 1. Effect of the concentration of nickel nanopowder in the 4.0% Mo/ZSM-5 catalyst on the yields of methane conversion products

Ni, wt %	Time of stream, min												
	20	60	100	140	180	220	260	300	340	380	420	460	500
	Yield of C_2H_6, %												
–	0.02	0.04	0.09	0.09	0.13	0.14	0.16	0.15	0.15	0.15	0.15	0.16	–
0.1	0.04	0.08	0.12	0.12	0.12	0.12	0.16	0.17	0.17	0.18	0.19	0.19	0.20
0.25	0.03	0.06	0.08	0.09	0.11	0.13	0.13	0.13	0.13	0.11	0.11	0.11	0.16
0.5	0.03	0.05	0.10	0.11	0.13	0.14	0.14	0.14	0.14	0.14	0.15	0.17	0.17
1.0	0.11	0.11	0.11	0.11	0.09	0.09	0.09	0.09	0.10	–	–	–	–
2.0	0.02	0.02	0.02	0.03	0.03	0.08	0.10	0.09	0.09	–	–	–	–
	Yield of C_2H_4, %												
–	0.15	0.24	0.26	0.30	0.32	0.37	0.43	0.44	0.54	0.61	0.73	0.80	0.83
0.1	0.15	0.22	0.23	0.26	0.29	0.31	0.30	0.32	0.35	0.37	0.39	0.40	0.41
0.2	0.16	0.23	0.26	0.27	0.27	0.32	0.32	0.34	0.36	0.36	0.40	0.42	0.45
0.5	0.15	0.23	0.24	0.25	0.29	0.30	0.32	0.36	0.39	0.40	0.44	0.47	0.50
1.0	0.12	0.23	0.32	0.38	0.47	0.57	0.61	0.67	0.67	–	–	–	–
2.0	–	–	0.13	0.22	0.36	0.40	0.52	0.54	0.57	–	–	–	–
	Yield of C_6H_6, %												
–	6.05	6.31	6.50	6.24	6.20	5.99	5.73	5.38	4.79	3.48	2.30	1.82	0.92
0.1	6.28	7.18	7.05	6.96	6.97	6.63	6.13	5.83	5.42	4.89	4.54	4.17	4.13
0.2	4.29	5.28	5.44	5.47	5.49	5.47	5.45	5.44	5.40	5.37	5.15	4.17	3.83
0.5	4.45	5.08	5.48	5.51	5.60	5.64	5.35	5.13	5.06	4.55	4.54	4.37	4.12
1.0	3.22	3.83	4.08	2.84	2.53	1.99	1.77	1.53	1.39	–	–	–	–
2.0	0.10	0.23	1.47	3.48	3.70	3.17	2.94	2.21	1.68	–	–	–	–
	Yield of $C_{10}H_8$, %												
–	3.42	3.70	3.60	3.41	3.26	2.99	2.56	2.32	2.07	1.89	0.91	–	–
0.1	3.02	3.34	3.35	3.34	3.26	3.28	3.44	3.38	3.40	3.78	3.58	3.38	3.16
0.25	3.08	2.86	2.91	2.99	2.78	2.83	2.80	2.80	2.80	2.71	2.49	2.48	2.30
0.5	3.23	2.75	2.68	2.69	2.73	2.71	2.65	2.64	2.59	2.86	2.74	2.72	2.65
1.0	4.47	3.93	3.57	2.73	2.28	1.89	1.45	1.20	0.88	–	–	–	–
2.0	–	–	0.06	0.93	1.31	1.41	1.31	1.21	0.92	–	–	–	–

weak and strong sites was observed. As a result, the total concentration of acid sites decreased from 924 to 830 μmol/g. The thermal desorption spectra of zeolites containing 1.0 and 2.0% Ni (not given in this paper) exhibited a third peak with maximum temperatures of 470 and 500°C, respectively, in the region of high temperatures. In this case, the total concentration of acid sites continued to decrease. Based on these results, we can conclude that, under the catalyst preparation conditions, new active centers were formed with the participation of Ni and these centers exhibited an enhanced strength.

After the introduction of Mo into the zeolite, the strength and concentration of both types of acid sites decreased; this fact suggests the interaction of the Brønsted acid sites of the zeolite with Mo species on calcination in the course of catalyst preparation and, probably, the formation of an $Al_2(MoO_4)_3$ phase. The addition of nickel nanopowder to the 4.0% Mo/ZSM-5 catalyst resulted in a change in its acid characteristics, which was especially pronounced at a higher

Table 2. Acid properties of the catalysts

Catalyst	T_{max} of species, °C			Concentration, μmol/g			
	T_I	T_{II}	T_{III}	C_I	C_{II}	C_{III}	C
ZSM-5	210	430	–	569	370	–	939
0.1% Ni/ZSM-5	210	430	–	562	362	–	924
0.5% Ni/ZSM-5	210	425	–	515	315	–	830
1.0% Ni/ZSM-5	210	415	470	492	248	60	800
2.0% Ni/ZSM-5	205	410	500	478	232	79	789
4.0%Mo/ZSM-5	200	380	–	510	304	–	814
(0.1% Ni–4.0% Mo)/ZSM-5	200	380	–	486	259	–	745
(0.5% Ni–4.0% Mo)/ZSM-5	200	375	–	444	155	–	599
(1.0% Ni–4.0% Mo)/ZSM-5	200	370	420	410	103	80	493

Note: T_I, T_{II}, and T_{III} are the peak temperatures for species I, II, and III, respectively; C_I, C_{II}, C_{III}, and C are the concentrations of acid sites in species I, II, and III and the total concentration, respectively.

Table 3. Changes in the weights of Ni–Mo-containing zeolites after methane dehydroaromatization

Catalyst	Weight changes, %		
	water	oxygen	coke
(0.1% Ni–4.0% Mo)/ZSM-5	–3.15 (120°C)	+0.05 (320°C)	–8.70 (558°C)
(0.25% Ni–4.0% Mo)/ZSM-5	–3.13 (120°C)	+0.05 (320°C)	–11.17 (575°C)
(0.5% Ni–4.0% Mo)/ZSM-5	–3.22 (120°C)	+0.04 (325°C)	–14.00 (585°C)

Note: Weight changes relative to the weight of pure (after coke burning up to 1000°C) catalysts are given. The corresponding peak temperatures in DTG curves are given in parentheses.

nickel content. Thus, the TD spectra of a sample of (1.0% Ni–4.0% Mo)/ZSM-5 exhibited the appearance of the third peak with a high energy of ammonia retention, and the concentration of acid sites of the high-temperature form was somewhat higher than that in the 1.0% Ni/ZSM-5 catalyst. This suggests the possible interaction of molybdenum and nickel with the formation of nickel–molybdenum compounds with various stoichiometric compositions; for example, this is characteristic of aluminum–nickel–molybdenum systems [9].

To reveal the effect of the concentration of Ni nanopowder in the 4.0% Mo/ZSM-5 catalyst on the character of carbon deposits formed in the course of methane dehydroaromatization, we studied the carbonized samples using thermal analysis.

The samples based on the 4.0% Mo/ZSM-5 catalyst with various nickel concentrations (0.1, 0.25, and 0.5 wt %) were treated with methane under the following identical conditions: reaction temperature, 750°C; CH_4 supply space velocity, 1000 h^{-1}; and τ = 500 min. From the results of thermal analysis (Table 3), it follows that the amounts of water and added oxygen were the same within the limits of experimental error, whereas the amount of coke considerably increased with increasing nickel nanopowder concentration.

As the concentration of nickel in the catalyst was increased from 0.1 to 0.5%, the maximum temperature of coke burning increased from 558 to 585°C, and the amount of coke increased by a factor of 1.6. The DTG curve for the catalyst containing 0.25% Ni exhibited a weak manifestation of a high-temperature shoulder, which increased and became clearly pronounced in the DTG and DTA curves at 650 and 660°C, respectively, for the (0.5% Ni–4.0% Mo)/ZSM-5 catalyst (Fig. 2). It is likely that the formation of a new coke species was due to the addition of nickel nanopowder to the Mo-containing zeolite; the higher the nanopowder content of the sample, the more clearly pronounced the high-temperature species. The electron-microscopic studies demonstrated that oxide MoO_3 particles of a two-dimensional morphology of size 10–50 nm were formed in the initial

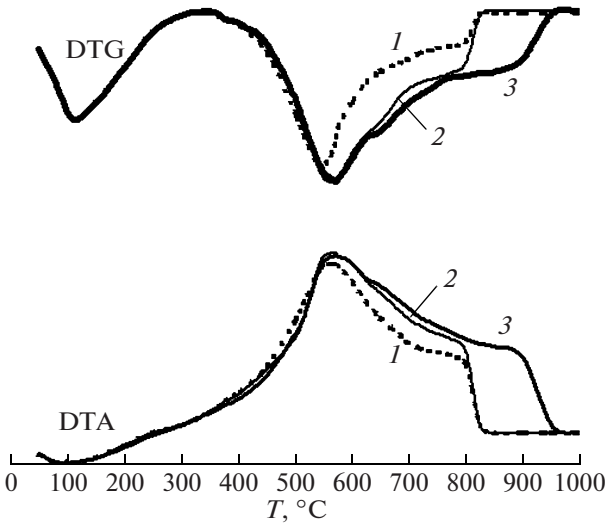

Fig. 2. Thermoanalytical profiles of the 4.0% Mo/ZSM-5 catalyst containing (*1*) 0.1, (*2*) 0.25, or (*3*) 0.5% Ni after treatment with methane (500 min) at $T = 750°C$.

samples of (Ni–4.0% Mo)/ZSM-5 (after calcination at 550°C) containing from 0.1 to 2.0% Ni (Fig. 3a). Note that, in the samples prepared by mixing Mo and Ni nanopowders with the zeolite, the supported component was dispersed incompletely. A portion of particles remained in a coarsely dispersed (to 50 nm in size) state (Fig. 3b).

In the samples after reaction, the particles of Ni and Mo compounds were detected, which were fundamentally different in morphology, composition, and arrangement in ZSM-5. First, note that Mo_2C carbide particles (of size 5–30 nm) weakly modified with 2–4 at % nickel occurred on the surface of zeolite crystals in all of the test samples of (Ni–Mo)/ZSM-5 (Fig. 4, spectrum *1*). However, even after the operation of the most stable (0.1% Ni–4.0% Mo)/ZSM-5 catalyst for 10 min, these particles were coated with a graphite-like carbon layer to 5 nm in thickness; that is, they rapidly deactivated (Fig. 5).

Oxidized Mo-containing clusters (Mo^{5+}) of size ~1 nm were observed in zeolite channels. The nature of these clusters, as well as surface molybdenum carbide particles, was analyzed in detail using TEM and EPR spectroscopy [10, 11]. The EDX analysis of zeolite regions with Mo clusters did not detect Ni as a constituent of them.

The TEM images show that carbon filaments from 10 to 50 nm in diameter (Fig. 7a) appeared in the (0.1% Ni–4.0% Mo)/ZSM-5 catalyst even after operation for 10 min. After $\tau = 500$ min, the amount of filamentous carbon considerably increased (Fig. 7b). Carbon in filaments had a tubular or conical structure of graphite-lake layers; metal particles occurred at the ends of growing filaments and within inner cavities (Fig. 8).

The mechanism of carbon filament formation on iron-family metals and their alloys with other metals was considered in detail in a number of publications [6, 11–13]. It was found that a metal or alloy particle interacts with a hydrocarbon to catalyze the growth of carbon through the formation of metastable carbides at the active site of the particle surface. Carbide degradation affords a metal and carbon atoms, which diffuse to the backside of the particle where a graphite-like phase is formed. According to this mechanism, the

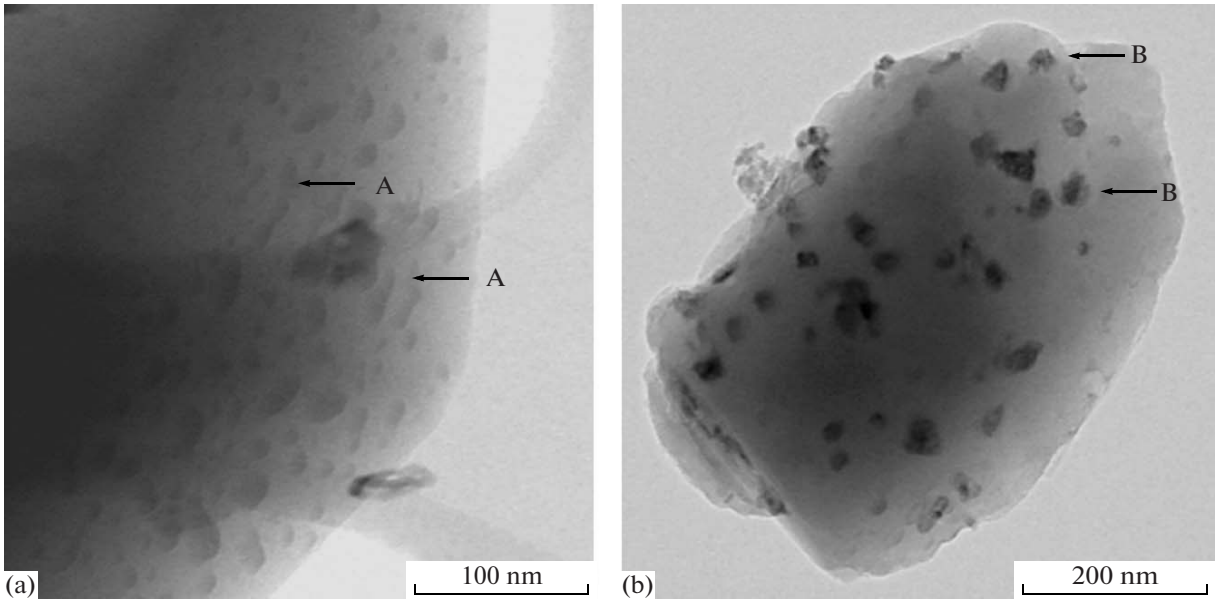

Fig. 3. HRTEM images of the (0.1% Ni–4.0% Mo)/ZSM-5 catalyst before reaction (after calcination at 550°C): (a) two-dimensional oxide particles and (b) coarsely dispersed MoO_3 and NiO particles.

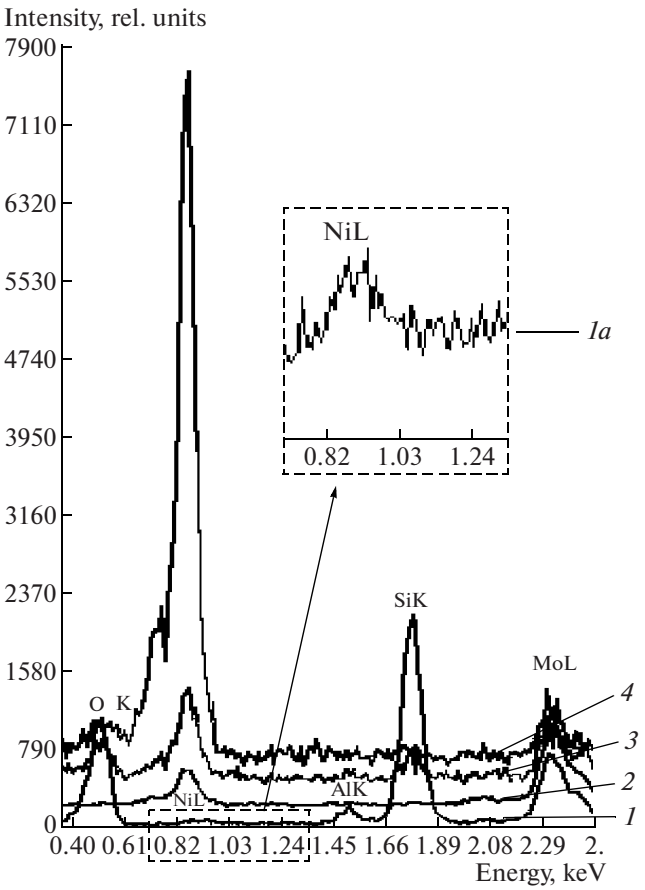

Fig. 4. EDX spectra of molybdenum compound particles: (*1*) molybdenum carbide particle weakly modified with nickel on the zeolite surface with the atomic ratio Mi/Mo = 4/96 (*1a*, a magnified fragment of the spectrum with the NiL line); (*2*, *3*) Ni–Mo alloy particles with different compositions at the end of carbon filaments (Ni/Mo = 20/80 and 50/50, respectively); (*4*) nickel particle within the channel of a carbon filament (Ni/Mo = 95/5).

front surface of a metal or alloy particle retains its catalytic activity for a long time in spite of the buildup of carbon.

An increase in the concentration of nickel in the zeolite did not change the nature of carbon products of the methane aromatization reaction: carbon filaments of the same morphology were formed in the catalysts containing 0.25 and 2.0% Ni. However, in this case, the amount of filamentous-morphology carbon and the sizes of filaments considerably increased. Figure 9 shows carbon filaments to 100 nm in diameter, which were observed in a large amount in the (2.0% Ni–4.0% Mo)/ZSM-5 catalyst after $\tau = 340$ nm. It can be seen that, in the deactivated catalyst, active component particles were blocked in the inner cavities of carbon filaments.

According to EDX data, the averaged composition of metal particles at the ends of carbon filaments corresponds to Ni–Mo alloys of different compositions. Thus, in particles of size ≈10 nm, the Ni/Mo atomic ratio is 50/50, whereas it is 20/80 in coarser particles (≈30 nm) (Fig. 4, spectra *2*, *3*). Small metal inclusions within tubular filaments torn from the backside of a particle contained mainly Ni and only an insignificant amount of Mo (Fig. 4, spectrum *4*). This suggests the inhomogeneous composition of the Ni–Mo alloy in an active particle with a shift of Mo toward the surface active for interaction with methane and a shift of Mo toward the back particle surface on which the growth of carbon occurs.

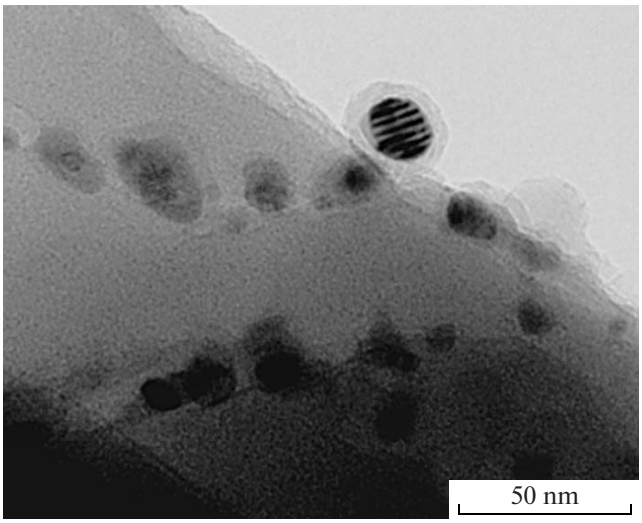

Fig. 5. Image of a Mo_2C particle on the surface of the (0.1% Ni–4.0% Mo)/ZSM-5 catalyst after 10-min methane dehydroaromatization reaction.

Thus, in the (Ni–Mo)/ZSM-5 catalysts, particles of different nature are formed: molybdenum clusters (of size ~1 nm) within zeolite channels, molybdenum carbide particles (5–30 nm) on the outer zeolite surface, and Ni–Mo alloy particles, on which carbon filaments grew under reaction conditions. The sizes of Mo and Ni nanoparticles were to 50 nm, although smaller particles were also detected in the catalyst. Molybdenum (VI) oxide has a comparatively low melting temperature (795°C); because of this, an elevated pressure of its vapor is generated at the stage of sample calcination in catalyst preparation. The condensation of MoO_3 vapor results in the penetration of Mo into the inner channels of the zeolite and the formation of disperse two-dimensional particles distributed over the zeolite surface. It is very likely that clusters within ZSM-5 channels are formed in the course of reaction with methane at 750°C. In addition, in the interaction of molybdenum with nickel particles on the zeolite surface, molybdenum carbide particles weakly modified with nickel (less than 5 at % Ni) and Ni–Mo alloy particles of different compositions, on which the growth of filamentous carbon occurred, can be formed.

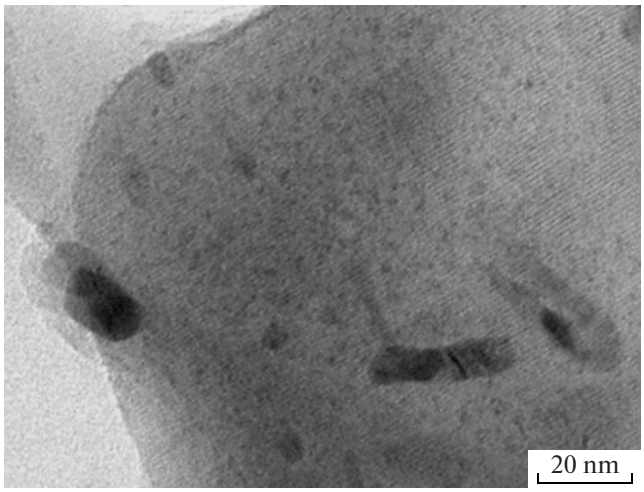

Fig. 6. Micrograph of inner Mo clusters in the zeolite and a surface particle of Mo_2C.

Previously, it was found that clusters within channels are responsible for the stable operation of Mo/ZSM-5 catalysts in methane aromatization [10, 11]. In this case, molybdenum clusters activate methane and the steps of conversion of intermediate products into benzene occur at the Brønsted acid sites of the zeolite either within channels or on the outer zeolite surface. With the participation of molybdenum clusters in the reaction, coke formation is insignificant, and it does not affect channels. Only highly dispersed graphite-like islands are formed on the outer surface of the zeolite after a long time of catalyst operation. Analogous clusters are observed in (Ni–Mo)/ZSM-5 catalysts (Ni, from 0.1 to 2.0%; Mo, 4.0%); nevertheless, nickel is not a component of these clusters. Therefore, it is believed that these clusters play the same role as in Mo/ZSM-5 catalysts. The observed carbonization of Ni–Mo carbide particles (of size 5–30 nm) on the zeolite surface even at the onset of reaction in the most stable of the catalysts—(0.1% Ni–4.0% Mo)/ZSM-5—excludes the possibility of increasing the stability of this catalyst.

At the same time, Ni–Mo alloy particles arranged at the ends of carbon filaments do not deactivate for a long time, which is even longer than the time of stable operation of Mo clusters within the zeolite. This is due to the fact that the reaction with methane occurs on the active frontal part of a particle, which is not covered with carbon, and the growth of a carbon filament occurs on its backside. Moreover, these particles are removed from the zeolite surface, which is also prone to coking. It should be taken into account that both Ni and Mo are the constituents of Ni–Mo alloy particles; this explains changes in the yields of the resulting products because of different functional roles of these metals in methane dehydroaromatization. The formation of metastable carbides (demonstrated in [6, 12, 13] for the mechanism of growth of carbon filaments) on the active sites of the Ni–Mo alloy particle surface, which are arranged at the ends of filaments, is consistent with a viewpoint on the carbide nature of methane activation sites in Mo-containing catalysts for methane aromatization.

Note that only a small addition of Ni (0.1%) afforded a stable catalyst, whereas the stability of the (0.25% Ni–4.0% Mo)/ZSM-5 catalyst was found lower. As follows from TEM and DTA data, the concentration of the formed coke increased as the nickel content of the zeolite was increased. There are published data indicating that the weight of filamentous carbon formed on Ni-containing catalysts can be

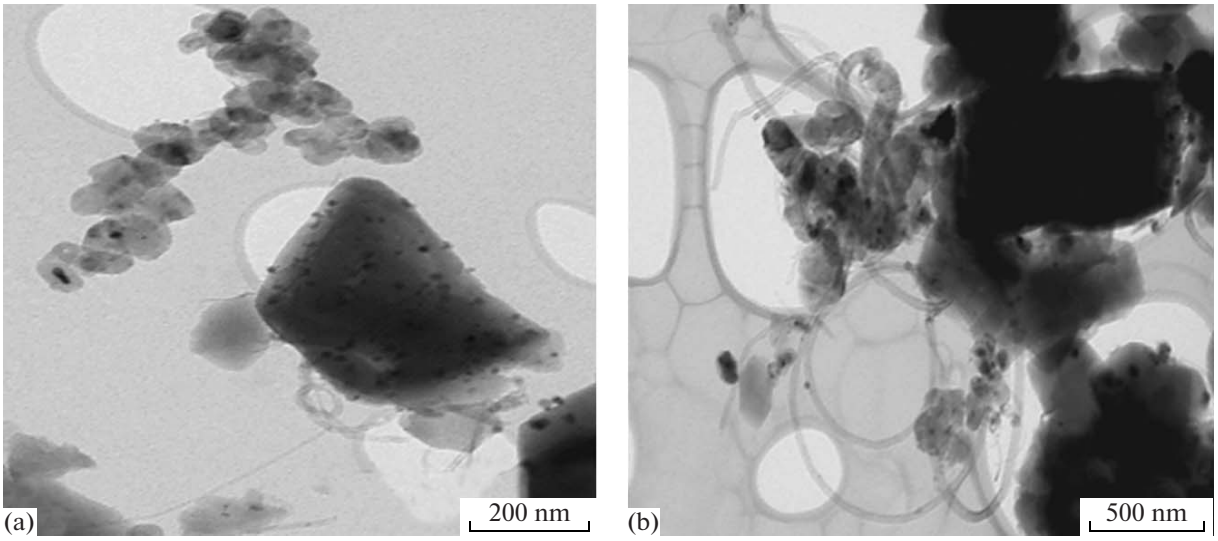

Fig. 7. Micrographs of carbon filaments in the (0.1% Ni–4.0% Mo)/ZSM-5 catalyst after (a) 10- or (b) 500-min methane dehydroaromatization reaction.

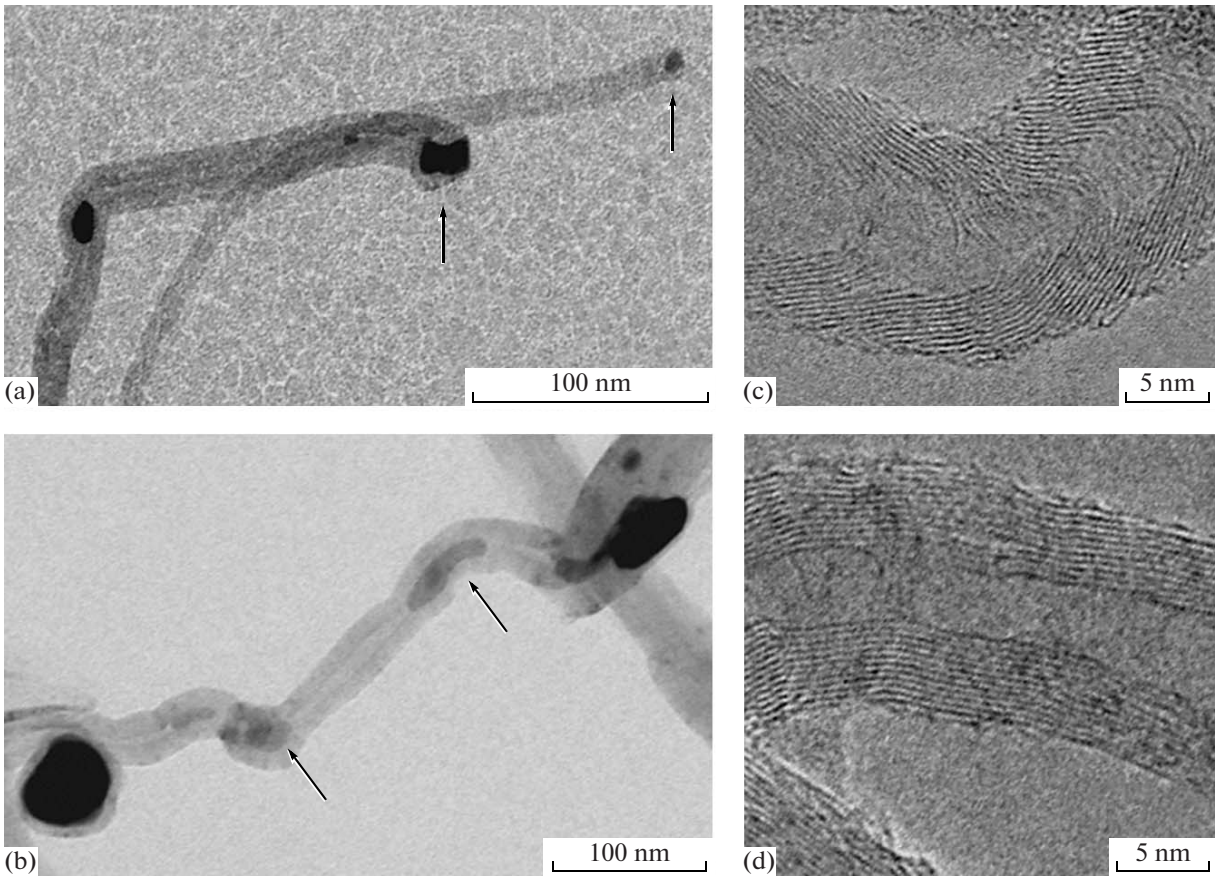

Fig. 8. Micrographs of the structures of carbon filaments in the samples of (Ni–Mo)/ZSM-5 catalysts after reaction: (a, b) metal particles are arranged at the ends and in the inner cavities of filaments, respectively (shown by arrows); (c) conical and (d) tubular structures of carbon filaments.

higher than the weight of the zeolite by factors of hundreds and thousands [6, 12, 13]. It is likely that a nickel content higher than a found optimum value (0.1 wt %) is responsible for the deactivation of this catalytic system because of pore blocking in the zeolite structure by filamentous carbon up to the formation of condensed coke deposits.

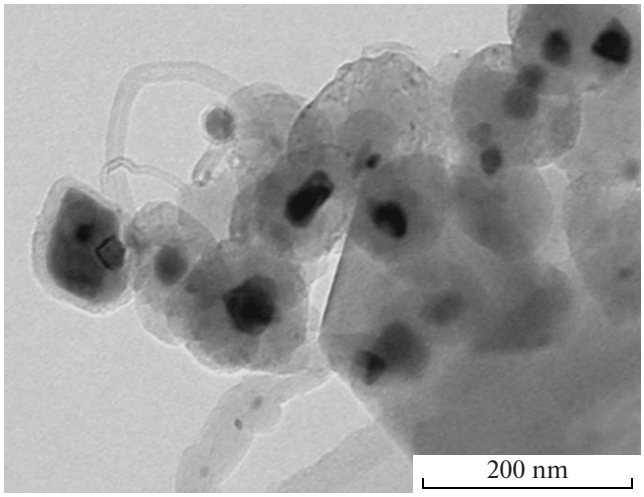

Fig. 9. Carbon filaments in the (2.0% Ni–4.0% Mo)/ZSM-5 catalyst after 340-min reaction.

Thus, we can conclude that the Mo-containing zeolite ZSM-5 with the addition of 0.1% Ni nanopowder is superior to other samples in not only catalytic activity but also stability. It exhibits advantages in the course of regeneration because a smaller amount of coke characterized by a lower degree of polycondensation is formed on this zeolite, and the less severe conditions of oxidative thermal treatment are required for the removal of this coke.

REFERENCES

1. Chen, L., Lin, L., and Xu, Z., *Catal. Lett.*, 1996, vol. 39, p. 169.
2. Wang, L., Xu, Y., Wong, S., Cui, W., and Guo, X., *Appl. Catal., A*, 1997, vol. 152, p. 173.
3. Liu, S., Dong, Q., Ohnishi, R., and Ichikawa, M., *Chem. Commun.*, 1997, p. 1445.
4. Wang Qiying and Lin Weiming, *J. Nat. Gas Chem.*, 2004, vol. 13, p. 91.

5. Gusev, A.I., *Nanokristallicheskie materialy: Metody polucheniya i svoistva* (Nanocrystalline Materials: Preparation and Properties), Yekaterinburg: Ural. Otd. Ross. Akad. Nauk, 1998.

6. Buyanov, R.A., *Zakoksovanie katalizatorov* (Coking of Catalysts), Moscow: Nauka, 1983.

7. Wang, D., Lunsford, J.H., and Rosynek, M.P., *J. Catal.*, 1997, vol. 169, p. 347.

8. Xu, Y. and Lin, L., *Appl. Catal., A*, 1999, vol. 188, p. 53.

9. Radchenko, E.D., Nefedov, B.K., and Aliev, R.R., *Promyshlennye katalizatory gidrogenizatsionnykh protsessov neftepererabotki* (Industrial Catalysts for Hydrogenation Processes in Petroleum Refining), Moscow: Khimiya, 1998.

10. Zaikovskii, V.I., Vosmerikov, A.V., Anufrienko, V.F., Korobitsyna, L.L., Kodenev, E.G., Echevskii, G.V., Vasenin, N.T., Zhuravkov, S.P., Ismagilov, Z.R., and Parmon, V.N., *Dokl. Akad. Nauk*, 2005, vol. 404, no. 4, p. 500 [*Dokl. Phys. Chem.* (Engl. Transl.), vol. 404, part 2, p. 201].

11. Matus, E.V., Ismagilov, I.Z., Sukhova, O.B., Zaikovskii, V.I., Tsikoza, L.T., Ismagilov, Z.R., and Moulijn, J.A., *Ind. Eng. Chem. Res.*, 2007, vol. 46, p. 4063.

12. Baker, R.T.K., Barber, M.A., Harris, P.S., Feates, F.S., and Waite, R.J.J., *J. Catal.*, 1972, vol. 26, p. 51.

13. Zaikovskii, V.I., Chesnokov, V.V., Buyanov, R.A., and Plyasova, L.M., *Kinet. Katal.*, 2000, vol. 41, no. 4, p. 593 [*Kinet. Catal.* (Engl. Transl.), vol. 41, no. 4, p. 538].